Electronic Supplementary Information

Fireproof Ultrastrong All-Natural Cellulose Nanofiber/Montmorillonite-Supported MXene Nanocomposites with Electromagnetic Interference Shielding and Thermal Management Multifunctional Applications

Rui Cheng[a], Ying Wu[b], Bin Wang[a, *], Jinsong Zeng[a], Jinpeng Li[a, *], Jun Xu[a], Wenhua Gao[a], and Kefu Chen[a]

[a]Plant Fiber Material Science Research Center, State Key Laboratory of Pulp and Paper Engineering, School of Light Industry and Engineering, South China University of Technology, Guangzhou 510640, China

[b]GuangDong Engineering Technology Research Center of Modern Fine Chemical Engineering, School of Chemical Engineering and Light Industry, Guangdong University of Technology, Guangzhou 510006, P. R. China

*Bin Wang. E-mail: febwang@scut.edu.cn

*Jinpeng Li. E-mail: ljp@scut.edu.cn

Characterizations

EMI shielding performances. The EMI shielding performances were measured through a vector network analyzer (PNA-N5244A, Agilent, USA) in the frequency range of 8.2-12.4 GHz (X-band). The transmission coefficient (*T*), reflection coefficient (*R*), absorption coefficient (*A*), total EMI SE (SE_T), reflection (SE_R), absorption (SE_A), and multiple internal reflections (SE_M) were calculated as follows:

$$R = |S_{11}|^2 = |S_{22}|^2, T = |S_{12}|^2 = |S_{21}|^2 (1)$$

$$A = 1 - R - T (2)$$

$$SE_R = -10\log(1 - R), SE_A = -10\log[T/(1 - R)] (3)$$

$$SE_T = SE_A + SE_R + SE_M (4)$$

Where the SE_M is negligible if the SE_T is higher than 10 dB. To further assess the EMI shielding capability, EMI SE/t is normalized to emiminate the effect of thickness. Furthermore, specific shielding effectiveness (SSE) and SSE/t taking into account the density and thickness are described as follows

$$SSE = EMI\ SE/density = dB \cdot cm^3 \cdot g^{-1} (5)$$

$$SSE/t = SSE/thickness = dB \cdot cm^2 \cdot g^{-1} (6)$$

EMI shielding efficiency (%), which represents the capability to block waves in terms of percentage, is achieved by the equation

$$\text{Shielding efficiency}(\%) = 100 - \left(\frac{1}{100^{\frac{SE}{10}}}\right) \times 100 (7)$$

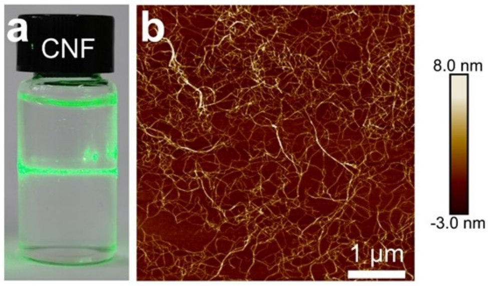

Fig. S1 (a) Digital image of CNF dispersion. (b) AFM image of CNFs.

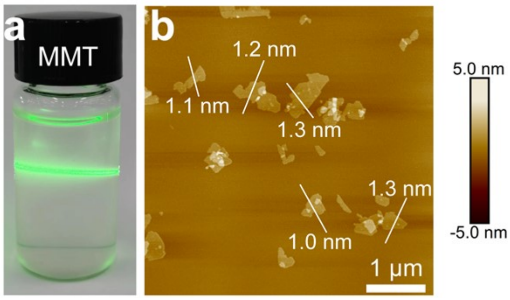

Fig. S2 Digital image of MMT dispersion. (b) AFM image of MMT nanosheets.

Fig. S3 Digital image of CNF/MMT dispersion.

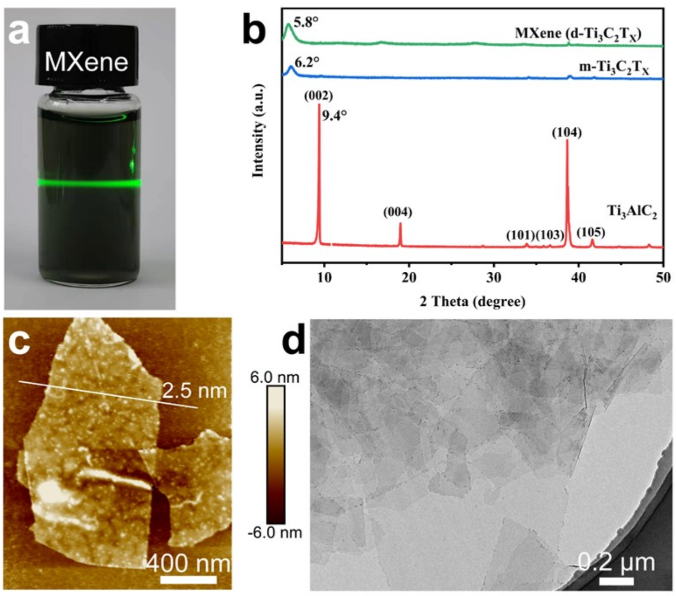

Fig. S4 (a) Digital image of MXene dispersion. (b) XRD patterns of Ti_3AlC_2 MAX, m-MXene, and MXene (d-$Ti_3C_2T_x$). (c) AFM and (d) TEM images of MXene nanosheets.

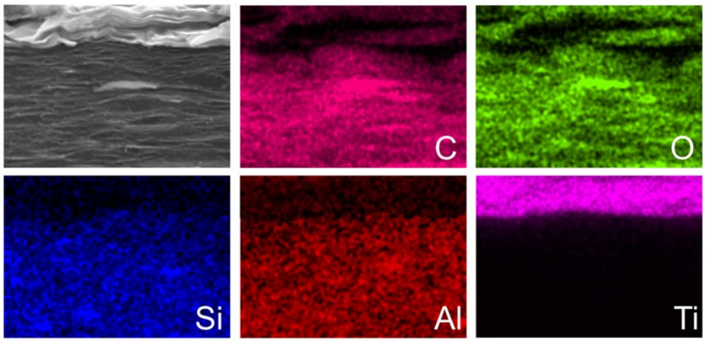

Fig. S5 SEM cross section and EDS mapping images of CMMP.

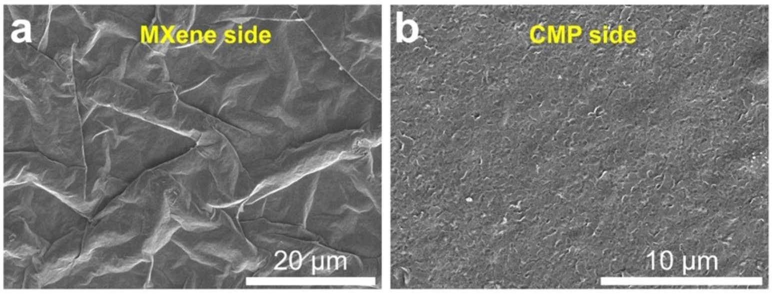

Fig. S6 SEM images of the CMMPs at (a) MXene side and (b) CMP side.

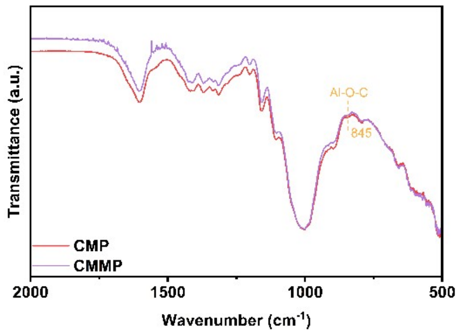

Fig. S7 FTIR spectra of CMP and CMMP. The CMP and CMMP spectrums show a weak peak at 844 cm^{-1}corresponding to the vibration of Al-O-C bond, which is formed by the hydroxyl groups of the CNFs with the Al of the MMT nanosheets.

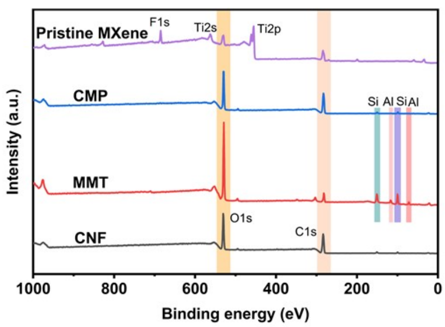

Fig. S8 XPS wide-scan spectra of CNF, MMT, CMP, and pristine MXene.

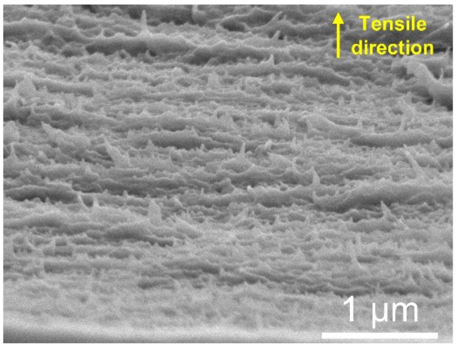

Fig. S9 SEM image of tensile fracture-surface morphologies of pure CNF papers.

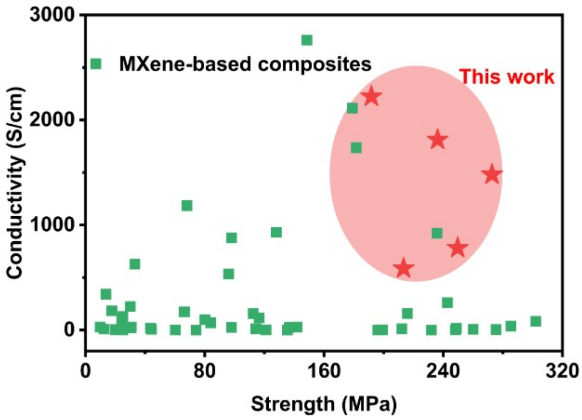

Fig. S10 Comparison of the electrical conductivity and tensile strength between the CMMPs and previously reported MXene-based nanocomposites.

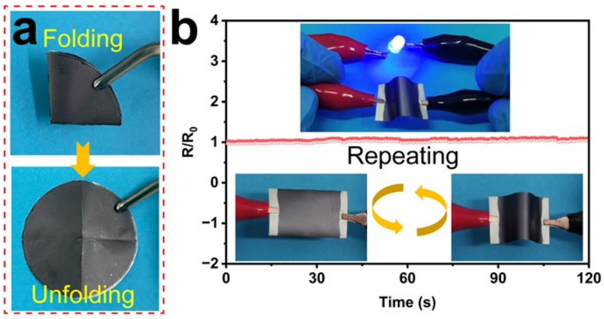

Fig. S11 Digital image showing great flexibility of the CMMP. (b) Real-time relative resistance of the CMMP during repeated bending and stretching.

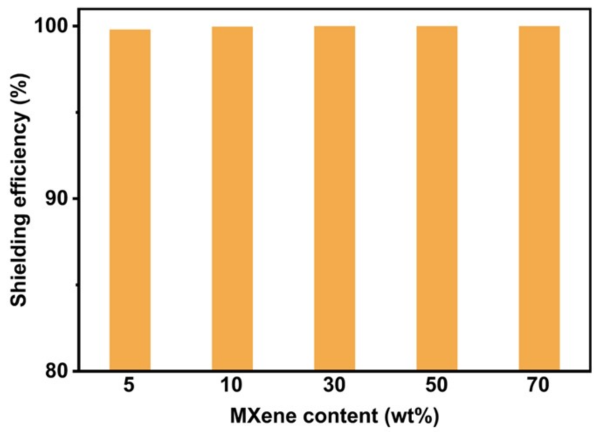

Fig. S12 The shielding efficiency of the CMMPs.

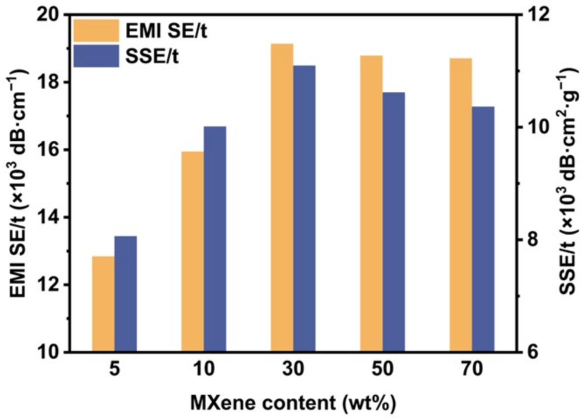

Fig. S13 EMI SE/t and SSE/t of the CMMPs.

HFSS simulation

In this study, all electromagnetic field simulations were performed by ANSYS HFSS 2021 R2 in the frequency domain. The size of the rectangular waveguide clamp is defined as a 22.86 × 10.16 × 40 mm ($x \times y \times z$). The model spaces are assigned the Floquet excitations and the master and slave boundaries. In brief, S1 and S2 corresponding to port 1 and 2 for the vector network analyzer are set up to generate electric field excitation and receive EM signals, respectively. The transmission mode of EM waves in the waveguide fixture is defined as the typical transverse electric wave, where the propagation directions of the electric field and magnetic field are vertical to each other. The *XY* plane of the cuboid is selected as the excitation face of the wave port and electromagnetic wave propagation along the *Z* direction. The rectangular waveguide boundary is set as a perfectly electric conductor (Perfect E). The mesh quality of the CMMPs is the default value. The solution step is set to frequency sweep, where the frequency type is the linear step from 8.2 GHz to 12.4 GHz with an interval of 0.1 GHz. The detailed parameters of the HFSS EMI simulation, such as electrical conductivity, thickness, permeability, excitation type, boundary conditions, etc. (Table S6†), are then put into the created model. The simulation results are achieved after executing the calculations.

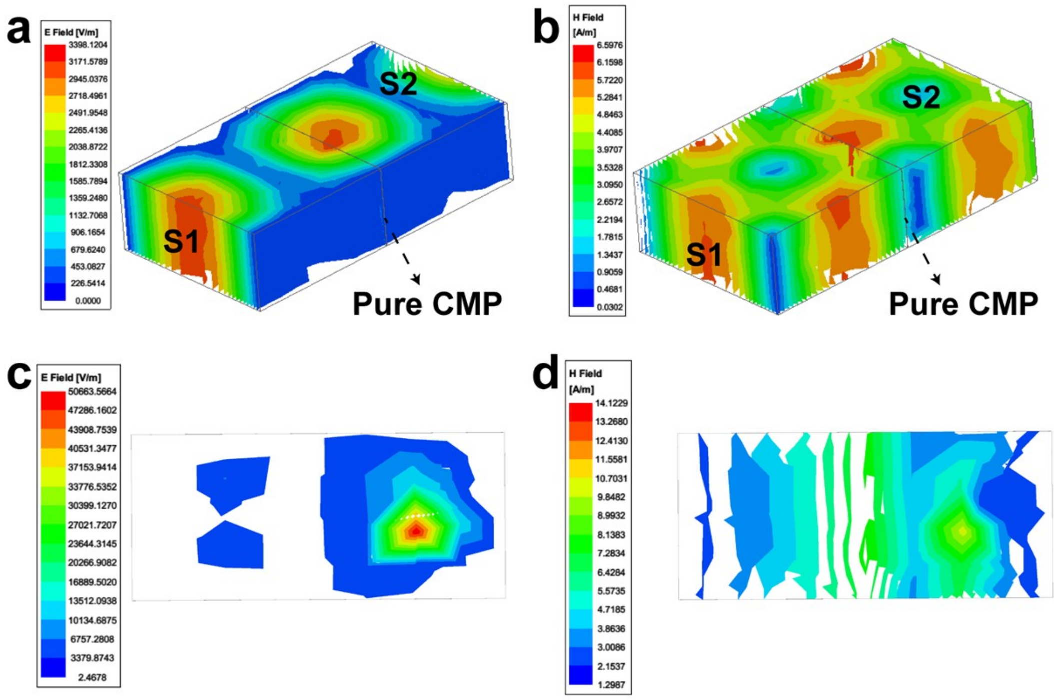

Fig. S14 Simulation diagram of (a) electric field distribution and magnetic field distribution in the rectangular waveguide clamp. (c) Electric field distribution and (d) magnetic field distribution of pure CMP.

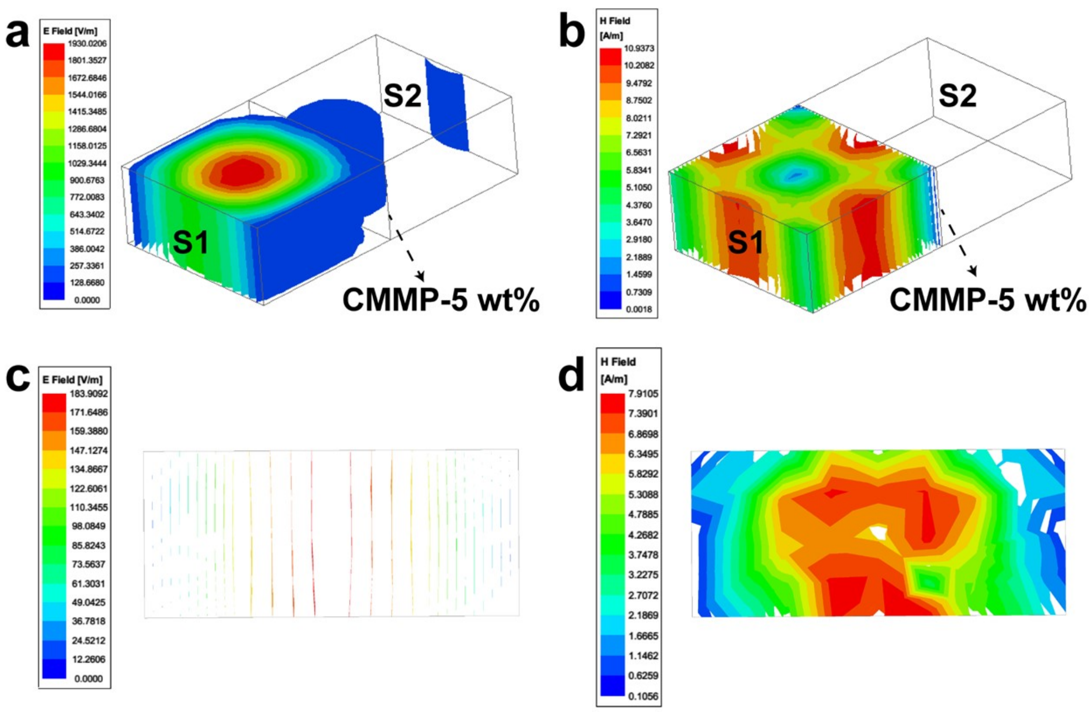

Fig. S15 Simulation diagram of (a) electric field distribution and magnetic field distribution in the rectangular waveguide clamp. (c) Electric field distribution and (d) magnetic field distribution of the CMMP-5 wt%.

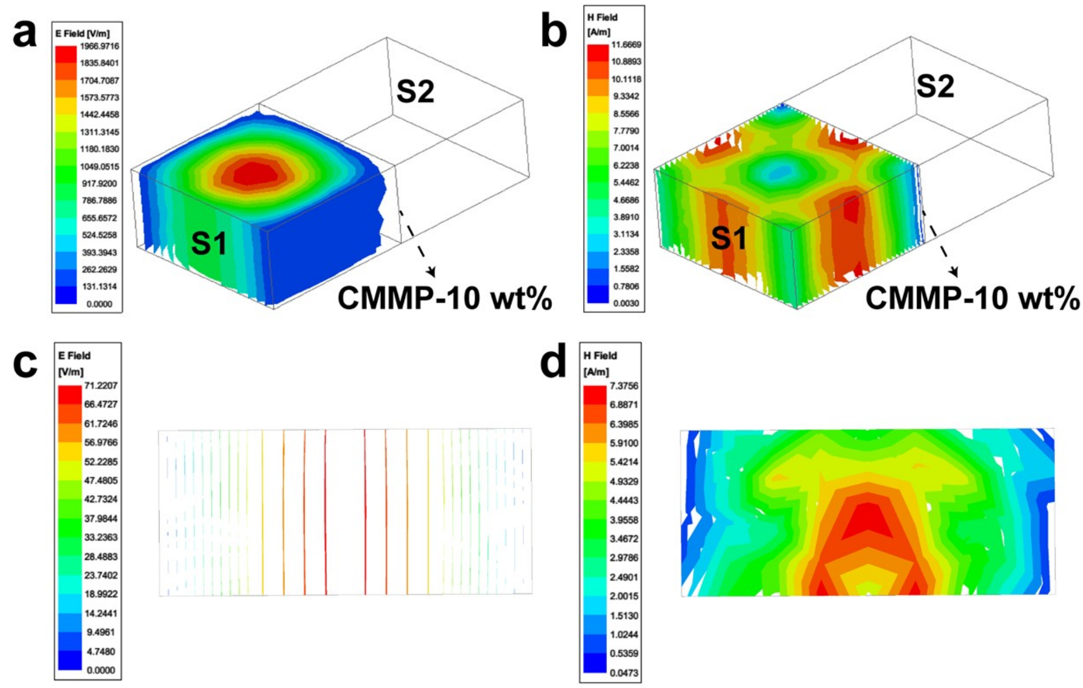

Fig. S16 Simulation diagram of (a) electric field distribution and magnetic field distribution in the rectangular waveguide clamp. (c) Electric field distribution and (d) magnetic field distribution of the CMMP-10 wt%.

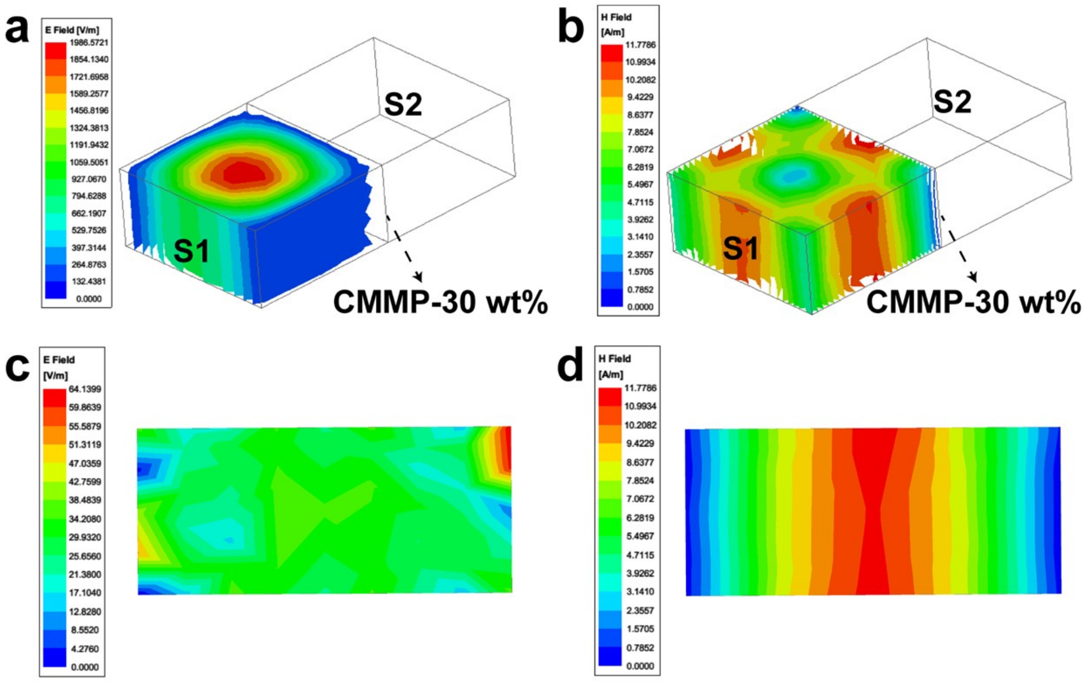

Fig. S17 Simulation diagram of (a) electric field distribution and magnetic field distribution in the rectangular waveguide clamp. (c) Electric field distribution and (d) magnetic field distribution of the CMMP-30 wt%.

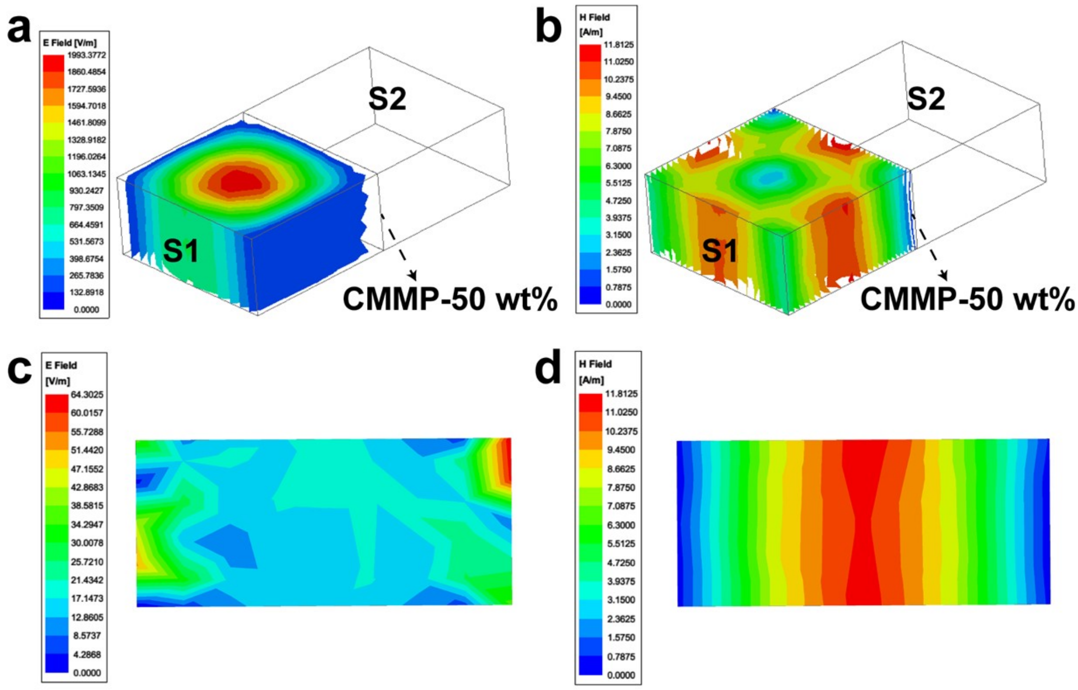

Fig. S18 Simulation diagram of (a) electric field distribution and magnetic field distribution in the rectangular waveguide clamp. (c) Electric field distribution and (d) magnetic field distribution of the CMMP-50 wt%.

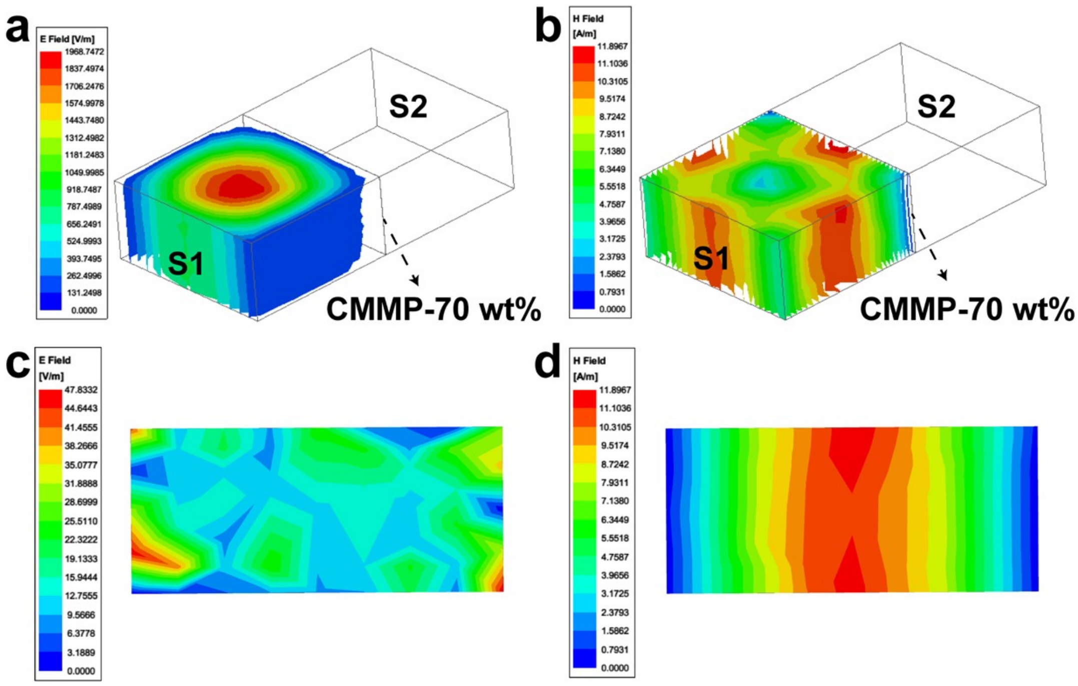

Fig. S19 Simulation diagram of (a) electric field distribution and magnetic field distribution in the rectangular waveguide clamp. (c) Electric field distribution and (d) magnetic field distribution of the CMMP-70 wt%.

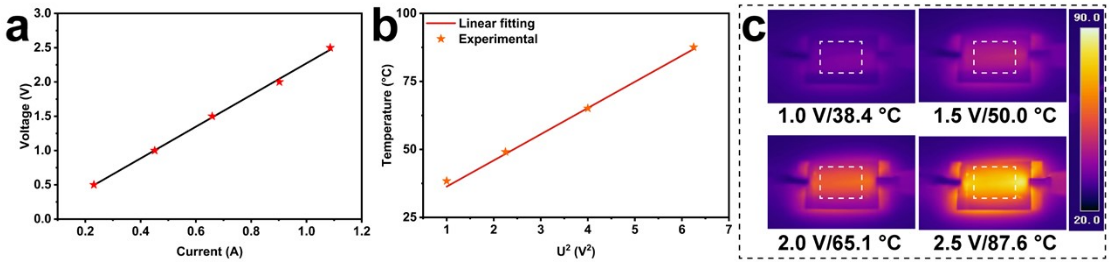

Fig. S20 (a) I-V curve of the CMMPs-10 at increased driving voltages. (b) Experimental data and linear fitting of saturation temperature *versus* U^2. (c) IR images under distinct voltages.

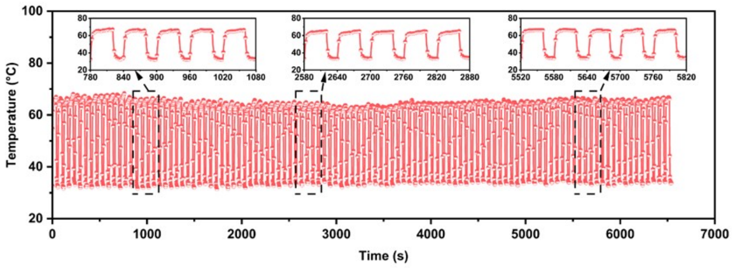

Fig. S21 Heating stability and repeatability of the CMMPs-10 upon repeated driving voltages.

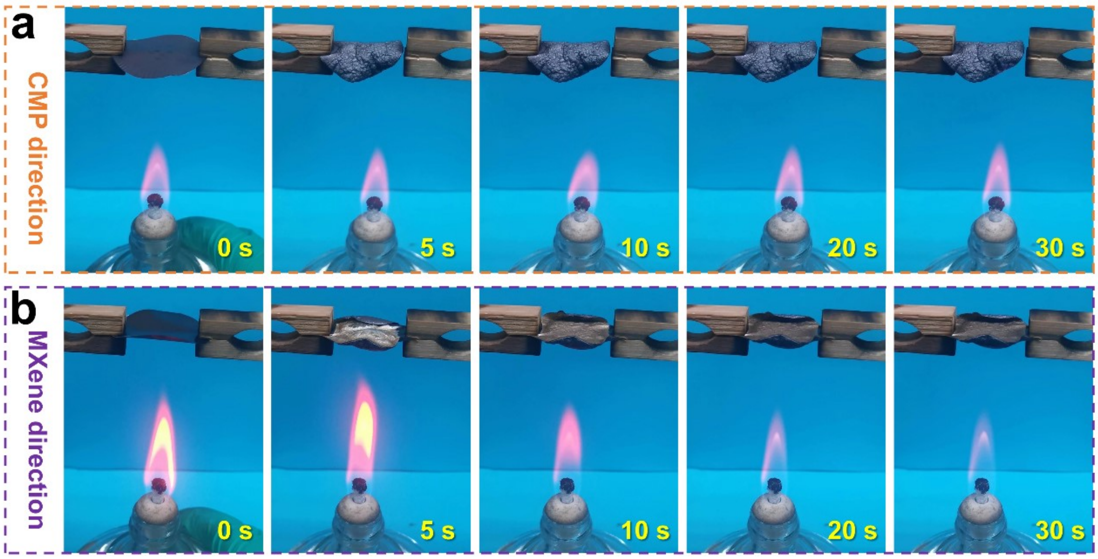

Fig. S22 Photographs of the CMMPs on a hot flame with time ranging from 0 to 30 s for (a) CMP direction and (b) MXene direction.

Table S1 Mechanical properties of previously reported MXene-based composite papers/films prepared by other strategies, including filtration, blade-coating, casting, in-situ biosynthesis, and layer-by-layer assembly[1-30].

Method	Materials	Strength (MPa)	Modulus (GPa)	Ref.
Filtration	MXene-CNF	135.4	3.8	1
Filtration	MXene-PVA	91.0	3.7	2
Filtration	MXene-CNF	212.0	7.0	3
Filtration	MXene-ANF	197.4	2	4
Filtration	MXene-ANF	116.7	5.0	5
Filtration	MXene-CNF-CNT	97.9	2.6	6
Filtration	MXene-ANF	131.3	8.3	7
Filtration	MXene-AgNWs-ANF	235.9	4.1	8
Filtration	MXene-ANF	166.0	4.8	9
Filtration	MXene-ANF	232.0	13.8	10
Filtration	MXene-CNF-AgNWs	118.0	5	11
Filtration	MXene-CNF	112.5	6	12
Filtration	MXene-CNF	114.4	4.1	13
Filtration	MXene-CNF	191.3	11.1	14
Filtration	MXene-CNF-polydopamine	237.1	8.5	15
Filtration	MXene-SA-MMT	110.1	3.5	16
Filtration	MXene-bacterial cellulose	252.2	9.0	17
Filtration	MXene-ANF	242.8	11.3	18
Filtration	MXene-PU	96.1	7.9	19
Filtration	MXene-PI	102.0	9	20
Filtration	MXene-xanthan	116.5	10.8	21
Filtration	MXene-Al^{3+}	83.2	7.4	22
Filtration	MXene-H^{+}	114.0	7.5	23
Blade-coating	MXene-ANF	198.8	6.1	24
Casting	MXene-PVA-BA	80.5	3.9	25
Casting	MXene-AgNWs-PVDF	39.2	0.46	26
In-situ biosynthesis	MXene-bacterial cellulose	297.5	5.1	27
Layer-by-layer assembly	MXene-CNF-bacterial cellulose	258.3	5.0	28
Layer-by-layer assembly	MXene-ANF	177.9	2.0	29
Layer-by-layer assembly	MXene-PVA-MMT	225.0	10.5	30
Successive filtration	**MXene-CNF-MMT**	**213.4**	**9.9**	**This work**
		249.7	**10.7**	

		272.7	**10.8**	
		236.2	**10.5**	

Table S2 Comparison of the electrical conductivity and tensile strength between the CMMPs and previously reported MXene-based composite papers/films[1-4, 8, 10, 18, 21, 24, 27, 31-37].

Method	Materials	Content (wt %)	Strength (MPa)	Conductivity (S/cm)	Ref.
Filtration	MXene-CNF-TA		260.0	6.2	31
			275.4	4.6	
			248.2	3.2	
			199.3	2.1	
Filtration	MXene-ANF	5	248.8	16.4	18
		10	285.4	37.6	
		20	302.1	82.9	
		40	242.8	260.7	
Filtration	MXene/CNF	50	135.4	0.097	1
		60	74.1	0.134	
		80	60.2	1.16	
		90	44.2	7.39	
Filtration	MXene-CNF	50	141.9	28.4	3
		40	212.2	12.1	
		30	196.1	0.3	
Filtration	MXene-CNF	50	68.0	1185.0	32
Filtration	MXene-ANF	40	136.6	24.8	4
		50	83.9	69.6	
		60	80.1	99.7	
		80	66.3	173.4	
		90	33.1	628.3	
Filtration	MXene-AgNWs-ANF	10	215.9	157.2	8
		20	235.9	922.0	
		40	181.6	1736.4	
		60	148.5	2760.7	
Filtration	MXene-xanthan	80	96.0	533.9	21
		66.67	116.5	115.3	
		57.14	114.3	12.1	
		50	121.1	1.9	
Filtration	MXene-chitosan	93	9.8	28.0	33
		90	30.7	27.6	
		86	43.5	18.2	
Filtration	MXene-PEDOT:PSS	87.5	13.7	340.5	34
		83.3	17.6	183.2	
		80	24.2	83.3	
		75	30.2	20.4	
Filtration	MXene-ANF	80	98.0	879.0	10

		10	232.0	0.2	
Filtration	MXene-PVA	90	30.0	224.3	2
		80	25.0	1.4	
In-situ biosynthesis	MXene-bacterial cellulose	76.9	112.5	156.3	27
Blade-coating	MXene-ANF	80	128.0	930.6	24
Layer-by-layer assembly	MXene-CNT	-	25.0	130.0	35
Layer-by-layer assembly	MXene-chitosan	14.7	20.0	3.9	36
		25.9	12.5	9.7	
Double cross-linking	MXene-CNF	70	179.0	2113.0	37
Successive filtration	**MXene-CNF-MMT**	**5**	**249.7**	**586.5**	**This work**
		10	**272.7**	**781.5**	
		30	**236.2**	**1480.2**	
		50	**191.8**	**1811.7**	
		70	**161.7**	**2222.5**	

Table S3 Shielding efficiency for the CMMPs

CMMPs	**Shielding efficiency (%)**
MXene-5 wt %	99.7992
MXene-10 wt %	99.9690
MXene-30 wt %	99.9975
MXene-50 wt %	99.9992
MXene-70 wt %	99.9998

Table S4 Summary of tensile strength and EMI SE/t of our CMMPs and other previously reported shielding materials[1, 3, 4, 6, 8, 12, 18, 21, 24, 34, 38-56].

Types	Materials	Strength (MPa)	EMI SE/t (dB/cm)	Ref.
MXene-based composites	MXene-ANF	248.8	12594.3	18
		285.4	14954.1	
		302.1	19870.7	
		242.8	19379.6	
	MXene-ANF-MMT	99.08	7375.8	38
		154.7	7289.5	
		130.2	7681.6	
		133.5	9853.6	
	MXene-CNF	44.2	5106.0	1
		60.2	3514.0	
		135.4	1497.0	
	MXene-CNF	212.0	10421.0	3
	MXene-CNF-CNT	97.9	10105.0	6
		94.9	6157.9	
	MXene-ANF	158.5	5539.1	4
	MXene-ANF	128.0	12973.0	24
		166.3	9150.0	
		210.8	7903.23	
	MXene-AgNWs-ANF	215.9	8658.5	8
		235.9	10688.9	
		181.6	11460.0	
		148.5	11446.4	
		79.8	8769.2	
	MXene-xanthan	121.1	17397.9	21
	MXene-PEDOT:PSS	24.16	16615.0	34
	MXene-CNF	112.5	11314.3	12
	MXene-carbon fiber-PU	170.0	808.0	39
	MXene-CNF-CNT	31.7	9000.0	40
		34.0	9083.3	
		34.8	9352.9	
		50.0	17083.3	
	MXene-AgNWs-CNF	137.0	20653.0	41
Carbon-based composites	CNT-sponge-epoxy	79.2	165.0	42
	CNT-CNF	27	3093.3	43
	CNT-WPU	2.3	1093.8	44
	CNT-PEO-cellulose	26.9	2333.3	45
	CNT-GCC	36.2	15000.0	46
	CNT-$CoFe_2o_4$-PVA	30.0	4526.0	47

	CNT-PVDF-Co	70.0	1143.0	48
	rGO-PEI	3.5	43.5	49
	rGO/PMMA	28.0	47.4	50
	Graphene papers	246.0	1900.0	51
	Graphene-TPU	58.0	1333.3	52
	Graphene pellet	22.0	12000.0	53
	rGO/PI	11.4	262.5	54
	GP-TiO-epoxy	75.0	3928.6	55
Metal-based composites	CPC-AgNW/textile	9.4	858.3	56
	MXene-CNF-MMT	**249.7**	**12843.9**	**This work**
		272.7	**15946.8**	
		236.2	**19140.8**	
		191.8	**18789.4**	
		161.7	**18708.7**	

Table S5 Summary of materials thickness and SSE/t of our CMMPs and other previously reported shielding materials[1, 3, 4, 6-8, 11, 12, 24, 34, 40, 57-77].

Types	Materials	Thickness (mm)	SSE/t (dB cm^2 g^{-1})	Ref.
MXene-based composites	MXene-CNF	0.167	1326	1
		0.074	2154	
		0.047	2647	
	MXene-CNF	0.035	4750	3
		0.047	4761	
	MXene-AgNWs-CNF	0.040	10901.6	11
	MXene-CNF	0.035	7029	12
	MXene-ANF	0.02	11200	4
	MXene-CNF-CNT	0.038	7874	6
	MXene-ANF	0.02137	8081.5	7
		0.01399	8814.5	
		0.01097	9555.7	
	MXene-AgNWs-ANF	0.041	7595.2	8
		0.045	8907.4	
		0.05	9317.1	
		0.056	8060.9	
		0.091	5379.9	
	MXene-ANF	0.04	10014	24
		0.031	8008.4	
	MXene-CNF-CNT	0.014	5305.7	40
		0.012	5140.8	
		0.017	8875.0	
		0.012	9316.4	
	MXene-carbon fiber	0.086	7723.9	57
	MXene-PEDOT:PSS	0.13	9169.5	34
	MXene-MMT	0.03	8381.5	58
		0.033	6336.2	
		0.045	6254.4	
	MXene-PVA	0.1	4770	59
		0.3	3867	
	MXene-PVA	0.027	9343	60
	MXene-wood	10	664.8	61
	MXene-PVA	3.49	4491.8	62
	MXene-rGO	2	8812.5	63
	MXene-CNT	3	8246.0	64
Carbon-based composites	CNT-PVDF	0.1	1430	65
	CNT/PEI	2	141	66
	MWCNT-WPU	2.3	2143	67

	MWCNT-GF-PDMS	15	5556	68
	MWCNT papers	0.6	3583	69
	rGO-PS	2.5	692	70
	Graphene-PEDOT:PSS	1.5	8040	71
	rGO-PU	20	332	72
	Carbon mat	0.29	1362	73
	CNT-CNF	2	2763.9	74
	MWCNT-cellulose	2.5	875.8	75
Metal-based composites	Stainless steel	4	27.5	76
	Ni fiber/PES	2.85	108.7	
	Ni filaments	2.85	164.9	
	Cu foil	0.01	7812	
	CF/Ni/PC	0.31	1376	77
	MXene-CNF-MMT	**0.022**	**10014.6**	**This work**
		0.024	**11095.8**	
		0.027	**10619.8**	
		0.03	**10366.8**	

Table S6 HFSS EMI simulation parameters of the CMMPs.

Parameter/Sample	5 wt%	10 wt%	30 wt%	50 wt%	70 wt%
Conductivity (S/cm)	586.5	781.5	1480.2	1811.7	2222.5
Thickness (mm)	0.001	0.002	0.004	0.007	0.010
Permeability	1				
Length (mm)	22.86				
Width (mm)	10.16				
Boundary conductions	Perfect E				
Mesh quality	Default				
Frequency (GHz)	8.2-12.4				
Step frequency (GHz)	0.1				
Excitation type	Wave port				
Source power (mw)	1				

Notes: Here, the thickness refers to the conductive layer thickness of the CMMPs.

References

1 W. T. Cao, F. F. Chen, Y. J. Zhu, Y. G. Zhang, Y. Y. Jiang, M. G. Ma and F. Chen, *ACS Nano*, 2018, **12**, 4583-4593.

2 Z. Ling, C. E. Ren, M. Q. Zhao, J. Yang, J. M. Giammarco, J. Qiu, M. W. Barsoum and Y. Gogotsi, *Proc. Nati. Acad. Sci*, 2014, **111**, 16676-16681.

3 Z. Zhan, Q. Song, Z. Zhou and C. Lu, *J. Mater. Chem. C*, 2019, **7**, 9820-9829.

4 F. Xie, F. Jia, L. Zhuo, Z. Lu, L. Si, J. Huang, M. Zhang and Q. Ma, *Nanoscale*, 2019, **11**, 23382-23391.

5 H. Wei, M. Wang, W. Zheng, Z. Jiang and Y. Huang, *Ceram. Int*, 2020, **46**, 6199-6204.

6 W. Cao, C. Ma, S. Tan, M. Ma, P. Wan and F. Chen, *Nano-Micro Lett.*, 2019, **11**, 72.

7 C. Lei, Y. Zhang, D. Liu, K. Wu and Q. Fu, *ACS Appl. Mater. Interfaces*, 2020, **12**, 26485-26495.

8 Z. Ma, S. Kang, J. Ma, L. Shao, Y. Zhang, C. Liu, A. Wei, X. Xiang, L. Wei and J. Gu, *ACS Nano*, 2020, **14**, 8368-8382.

9 Z. Zhang, S. Yang, P. Zhang, J. Zhang, G. Chen and X. Feng, *Nat. Commun.*, 2019, **10**, 2920.

10 C. Weng, T. Xing, H. Jin, G. Wang, Z. Dai, Y. Pei, L. Liu and Z. Zhang, *Compos. Part A: Appli. Sci. Manuf.*, 2020, **135**, 105927.

11 B. Zhou, Q. Li, P. Xu, Y. Feng, J. Ma, C. Liu and C. Shen, *Nanoscale*, 2021, **13**, 2378-2388.

12 B. Zhou, Z. Zhang, Y. Li, G. Han, Y. Feng, B. Wang, D. Zhang, J. Ma and C. Liu, *ACS Appl. Mater. Interfaces*, 2020, **12**, 4895-4905.

13 E. Jiao, K. Wu, Y. Liu, M. Lu, Z. Hu, B. Chen, J. Shi and M. Lu, *Compos. Part A: Appli. Sci. Manuf.*, 2021, **146**, 106417.

14 E. Jiao, K. Wu, Y. Liu, M. Lu, H. Zhang, H. Zheng, C. A. Xu, J. Shi and M. Lu, *Compos. Part A: Appli. Sci. Manuf.*, 2021, **143**, 106290.

15 J. Cao, Z. Zhou, Q. Song, K. Chen, G. Su, T. Zhou, Z. Zheng, C. Lu and X. Zhang, *ACS Nano*, 2020, **14**, 7055-7065.

16 Y. Zhang, W. Cheng, W. Tian, J. Lu, L. Song, K. M. Liew, B. Wang and Y. Hu, *ACS Appl. Mater. Interfaces*, 2020, **12**, 6371-6382.

17 X. Xu, S. Wu, J. Cui, L. Yang, D. Liu, Y. Zhang, X. Chen, K. Wu and D. Sun, *Cellulose*, 2021, **28**, 3311-3325.

18 J. Hu, C. Liang, J. Li, C. Lin, Y. Liang and D. Dong, *ACS Appl. Mater. Interfaces*, 2022, **14**, 33817-33828.

19 Z. Liu, W. Wang, J. Tan, J. Liu, M. Zhu, B. Zhu and Q. Zhang, *J. Mater. Chem. C*, 2020, **8**, 7170-7180.

20 Y. Zhu, X. Zhao, Q. Peng, H. Zheng, F. Xue, P. Li, Z. Xu and X. He, *Nanoscale Advances*, 2021, **3**, 5683-5693.

21 Y. Sun, R. Ding, S. Y. Hong, J. Lee, Y. K. Seo, J. D. Nam and J. Suhr, *Chem. Eng. J.*, 2021, **410**, 128348.

22 Z. Liu, Y. Zhang, H. B. Zhang, Y. Dai, J. Liu, X. Li and Z. Z. Yu, *J. Mater. Chem. C*, 2020, **8**, 1673-1678.

23 H. Chen, Y. Wen, Y. Qi, Q. Zhao, L. Qu and C. Li, *Adv. Funct. Mater.*, 2020, **30**, 1906996.

24 J. Wang, X. Ma, J. Zhou, F. Du and C. Teng, *ACS Nano*, 2022, **16**, 6700-6711.

25 J. H. Woo, N. H. Kim, S. I. Kim, O. K. Park and J. H. Lee, *Compos. Part B: Eng.*, 2020, **199**, 108205.

26 H. Cheng, Y. Pan, Q. Chen, R. Che, G. Zheng, C. Liu, C. Shen and X. Liu, *Adv. Compos. Hybrid Mater.*, 2021, **4**, 505-513.

27 Y. Wan, P. Xiong, J. Liu, F. Feng, X. Xun, F. M. Gama, Q. Zhang, F. Yao, Z. Yang, H. Luo and Y. Xu, *ACS Nano*, 2021, **15**, 8439-8449.

28 Z. Zhou, Q. Song, B. Huang, S. Feng and C. Lu, *ACS Nano*, 2021, **15**, 12405-12417.

29 D. Hu, S. Wang, C. Zhang, P. Yi, P. Jiang and X. Huang, *Nano Research*, 2021, **14**, 2837-2845.

30 J. Lipton, G. M. Weng, M. Alhabeb, K. Maleski, F. Antonio, J. Kong, Y. Gogotsi and A. D. Taylor, *Nanoscale*, 2019, **11**, 20295-20300.

31 J. Wei, S. Jia, J. Wei, C. Ma and Z. Shao, *ACS Appl. Mater. Interfaces*, 2021, **13**, 38700-38711.

32 W. Tian, A. VahidMohammadi, M. S. Reid, Z. Wang, L. Ouyang, J. Erlandsson, T. Pettersson, L. Wågberg, M. Beidaghi and M. M. Hamedi, *Adv. Mater.*, 2019, **31**, 1902977.

33 C. Hu, F. Shen, D. Zhu, H. Zhang, J. Xue and X. Han, *Frontiers in Energy Research*, 2017, **4**.

34 R. Liu, M. Miao, Y. Li, J. Zhang, S. Cao and X. Feng, *ACS Appl. Mater. Interfaces*, 2018, **10**, 44787-44795.

35 G. M. Weng, J. Li, M. Alhabeb, C. Karpovich, H. Wang, J. Lipton, K. Maleski, J. Kong, E. Shaulsky, M. Elimelech, Y. Gogotsi and A. D. Taylor, *Adv. Funct. Mater.*, 2018, **28**, 1803360.

36 Z. Tan, H. Zhao, F. Sun, L. Ran, L. Yi, L. Zhao and J. Wu, *Compos. Part A: Appli. Sci. Manuf.*, 2022, **155**, 106809.

37 N. Wu, Z. Zeng, N. Kummer, D. Han, R. Zenobi and G. Nyström, *Small Methods*, 2021, **5**, 2100889.

38 W. Dang, Z. Liu, L. Wang, Y. Chen, M. Qi and Q. Zhang, *Nanoscale*, 2022, **14**, 11305-11315.

39 N. Duan, Z. Shi, Z. Wang, B. Zou, C. Zhang, J. Wang, J. Xi, X. Zhang, X. Zhang and G. Wang, *Materials & Design*, 2022, **214**, 110382.

40 B. Wang, Y. Li, W. Zhang, J. Sun, J. Zhao, Y. Xu, Y. Liu, H. Guo and D. Zhang, *Carbohyd. Polym.*, 2022, **286**, 119302.

41 F. Zhang, P. Ren, Z. Guo, J. Wang, Z. Chen, Z. Zong, J. Hu, Y. Jin and F. Ren, *J. Mater. Sci. Technol*, 2022, **129**, 181-189.

42 Y. Chen, H. B. Zhang, Y. Yang, M. Wang, A. Cao and Z. Z. Yu, *Adv. Funct. Mater.*, 2016, **26**, 447-455.

43 H. Zhang, X. Sun, Z. Heng, Y. Chen, H. Zou and M. Liang, *Ind. Eng. Chem. Res.*, 2018, **57**, 17152-17160.

44 Z. Zeng, M. Chen, H. Jin, W. Li, X. Xue, L. Zhou, Y. Pei, H. Zhang and Z. Zhang, *Carbon*, 2016, **96**, 768-777.

45 L. Q. Zhang, B. Yang, J. Teng, J. Lei, D. X. Yan, G. J. Zhong and Z. M. Li, *J. Mater. Chem. C*, 2017, **5**, 3130-3138.

46 M. Yang, Q. Wei, J. Li, Y. Wang, H. Guo, L. Gao, L. Huang, X. He, Y. Li and Y. Yuan, *Adv. Mater. Interfaces*, 2020, **7**, 1901815.

47 G. H. Lim, S. Woo, H. Lee, K. S. Moon, H. Sohn, S. E. Lee and B. Lim, *ACS Appl. Mater. Interfaces*, 2017, **9**, 40628-40637.

48 X. Li, S. Zeng, S. E, L. Liang, Z. Bai, Y. Zhou, B. Zhao and R. Zhang, *ACS Appl. Mater. Interfaces*, 2018, **10**, 40789-40799.

49 J. Ling, W. Zhai, W. Feng, B. Shen, J. Zhang and W. g. Zheng, *ACS Appl. Mater. Interfaces*, 2013, **5**, 2677-2684.
50 H. B. Zhang, Q. Yan, W. G. Zheng, Z. He and Z. Z. Yu, *ACS Appl. Mater. Interfaces*, 2011, **3**, 918-924.
51 W. L. Song, L. Z. Fan, M. S. Cao, M. M. Lu, C. Y. Wang, J. Wang, T. T. Chen, Y. Li, Z. L. Hou, J. Liu and Y. P. Sun, *J. Mater. Chem. C*, 2014, **2**, 5057-5064.
52 B. Shen, Y. Li, D. Yi, W. Zhai, X. Wei and W. Zheng, *Carbon*, 2017, **113**, 55-62.
53 L. Zhang, N. T. Alvarez, M. Zhang, M. Haase, R. Malik, D. Mast and V. Shanov, *Carbon*, 2015, **82**, 353-359.
54 Y. Li, X. Pei, B. Shen, W. Zhai, L. Zhang and W. Zheng, *RSC Advances*, 2015, **5**, 24342-24351.
55 A. Kumar, R. Anant, K. Kumar, S. S. Chauhan, S. Kumar and R. Kumar, *RSC Advances*, 2016, **6**, 113405-113414.
56 L. C. Jia, G. Zhang, L. Xu, W. J. Sun, G. J. Zhong, J. Lei, D. X. Yan and Z. M. Li, *ACS Appl. Mater. Interfaces*, 2019, **11**, 1680-1688.
57 K. Wang, C. Chen, Q. Zheng, J. Xiong, H. Liu, L. Yang, Y. Chen and H. Li, *Carbon*, 2022, **197**, 87-97.
58 L. Li, Y. Cao, X. Liu, J. Wang, Y. Yang and W. Wang, *ACS Appl. Mater. Interfaces*, 2020, **12**, 27350-27360.
59 H. Xu, X. Yin, X. Li, M. Li, S. Liang, L. Zhang and L. Cheng, *ACS Appl. Mater. Interfaces*, 2019, **11**, 10198-10207.
60 X. Jin, J. Wang, L. Dai, X. Liu, L. Li, Y. Yang, Y. Cao, W. Wang, H. Wu and S. Guo, *Chem. Eng. J.*, 2020, **380**, 122475.
61 M. Zhu, X. Yan, H. Xu, Y. Xu and L. Kong, *Carbon*, 2021, **182**, 806-814.
62 Z. Guo, Y. Li, P. Jin, T. Zhang, Y. Zhao, Y. Ai, H. Xiu, Q. Zhang and Q. Fu, *Polymer*, 2021, **230**, 124101.
63 S. Zhao, H. B. Zhang, J. Q. Luo, Q. W. Wang, B. Xu, S. Hong and Z. Z. Yu, *ACS Nano*, 2018, **12**, 11193-11202.
64 P. Sambyal, A. Iqbal, J. Hong, H. Kim, M.-K. Kim, S. M. Hong, M. Han, Y. Gogotsi and C. M. Koo, *ACS Appl. Mater. Interfaces*, 2019, **11**, 38046-38054.
65 B. Zhao, C. Zhao, R. Li, S. M. Hamidinejad and C. B. Park, *ACS Appl. Mater. Interfaces*, 2017, **9**, 20873-20884.
66 D. Feng, Q. Wang, D. Xu and P. Liu, *Compos. Sci. Technol.*, 2019, **182**, 107753.
67 Z. Zeng, H. Jin, M. Chen, W. Li, L. Zhou and Z. Zhang, *Adv. Funct. Mater.*, 2016, **26**, 303-310.
68 X. Sun, X. Liu, X. Shen, Y. Wu, Z. Wang and J. K. Kim, *Compos. Part A: Appli. Sci. Manuf.*, 2016, **85**, 199-206.
69 A. Chaudhary, S. Kumari, R. Kumar, S. Teotia, B. P. Singh, A. P. Singh, S. K. Dhawan and S. R. Dhakate, *ACS Appl. Mater. Interfaces*, 2016, **8**, 10600-10608.
70 D. X. Yan, H. Pang, B. Li, R. Vajtai, L. Xu, P. G. Ren, J. H. Wang and Z. M. Li, *Adv. Funct. Mater.*, 2015, **25**, 559-566.
71 Y. Wu, Z. Wang, X. Liu, X. Shen, Q. Zheng, Q. Xue and J. K. Kim, *ACS Appl. Mater. Interfaces*, 2017, **9**, 9059-9069.
72 B. Shen, Y. Li, W. Zhai and W. Zheng, *ACS Appl. Mater. Interfaces*, 2016, **8**, 8050-8057.

73 X. Hong and D. D. L. Chung, *Carbon*, 2017, **111**, 529-537.
74 G. Zhu, L. Giraldo Isaza, B. Huang and A. Dufresne, *ACS Sustainable Chemistry & Engineering*, 2022, **10**, 2397-2408.
75 H. D. Huang, C. Y. Liu, D. Zhou, X. Jiang, G. J. Zhong, D. X. Yan and Z. M. Li, *J. Mater. Chem. A*, 2015, **3**, 4983-4991.
76 F. Shahzad, M. Alhabeb, C. B. Hatter, B. Anasori, S. M. Hong, C. M. Koo and Y. Gogotsi, *Science*, 2016, **353**, 1137-1140.
77 D. Xing, L. Lu, K. S. Teh, Z. Wan, Y. Xie and Y. Tang, *Carbon*, 2018, **132**, 32-41.